System Fragility Curves for a Long Multi-Frame Bridge under Differential Support Motions

Jong-Su Jeon
Postdoctoral Researcher, School of Civil and Environmental Engineering, Georgia Institute of Technology, Atlanta, USA

Abdollah Shafieezadeh
Assistant Professor, Dept. of Civil, Environmental and Geodetic Engineering, The Ohio State University, Columbus, USA

Reginald DesRoches
Karen and John Huff School Chair and Professor, School of Civil and Environmental Engineering, Georgia Institute of Technology, Atlanta, USA

ABSTRACT: The paper presents the seismic fragility assessment of a long multi-frame bridge subjected to differential support motions. For this purpose, a bridge experiencing the 1992 Landers earthquake is first chosen as the subject bridge and its numerical model is created using OpenSees. Nonlinear time-history analyses for the model under both uniform and multi-support motions recorded during the earthquake are performed and the simulated deck deformations are compared with the recorded sensor data. The results highlight the significance of multi-support motions along with an appropriate bridge model. For the derivation of fragility curves of the bridge, the conditional simulation of spatially variable ground motions is undertaken to obtain a set of acceleration time histories at different supports, which are converted into a set of displacement time histories. A set of analyses for the simulated motions are conducted on statistical realizations of the bridge model reflecting material and structural uncertainties to monitor the seismic demand of components. Accordingly, a new analytical formulation for the intensity measure is introduced to consider the spatial correlation of ground motions. Given the demands and limit states, component fragility curves are developed on the basis of the closed form, and system fragility curves are developed using Monte Carlo simulation. The fragility results reveal that a reduction in the average shear wave velocity results in an increase in the exceedance probabilities at higher limit states and thus the increase of bridge vulnerability.

1. INTRODUCTION

During earthquakes, ground motions that excite multiple supports of large structures such as dams, pipelines, and bridges may differ significantly. Thus, realistic seismic assessment of these structures must account for the spatial variation of ground motions over the entire length of such a structure. In other words, input motions that are imposed at the supports not only should possess realistic characteristics individually, but also should be properly correlated with each other. Nevertheless, current seismic design codes and methods of practice and risk assessment do not properly account for the effect of spatially variable ground motions on the response of large, geographically distributed structures such as multi-frame bridges. Spatial variation in ground motion characteristics in the time and frequency domains may cause damage to structures.

This study focuses on assessing the seismic vulnerability of a long multi-frame concrete box-girder bridge that experienced different motions at different supports. A conditional stochastic

random process is used to simulate multi-support motions that are conditioned on a set of ground motions recorded at a specific site (Vanmarcke et al. 1993, Liao and Zerva 2006). A detailed numerical model of the bridge is created using OpenSees (McKenna et al. 2010). Nonlinear time history analyses (NTHAs) for the bridge under both uniform and multi-support motions are performed, and the simulated results are compared with sensor data that were recorded at several locations of the subject bridge during the 1992 Landers earthquake. A comparison of the simulated responses with these recorded sensor data highlights the importance of multi-support excitation analysis along with a proper bridge model. Using a set of NTHAs, an intensity measure (IM) accounting for the spatial variation of ground motions is developed for component demand models. These demand models can be employed to generate component and system fragilities that express the likelihood of structural damage for various ranges of ground motion intensities.

2. BRIDGE MODEL AND VALIDATION

The bridge chosen in this study is the Northwest Connector, which is located at a freeway interchange in Colton, California. The bridge was retrofitted and instrumented a few months before it was struck by the 1992 Landers earthquake. As illustrated in Figure 1, the subject bridge is a 774 m long, curved concrete box-girder bridge with 16 spans supported by 15 single column bents and two diaphragm abutments. The overall bridge system comprises six frames, connected at the five in-span hinges. The frames have a reinforced and prestressed box girder superstructure with 12.5 m width and 2.45 m depth supported by two to four single column bents. The original column has a 2.44 m by 1.68 m octagonal section, while the retrofitted column has an elliptical cross-section with overall dimensions of 2.69 m by 2.06 m. For the retrofitted columns, a 12.7 mm thick steel casing in an elliptical shape was used to improve the confinement, shear strength, and flexural ductility of the columns; full-height steel jackets were used to encase the columns at 12 of the 15 bents; and partial-height steel jackets were used for Bents 8, 12, and 14. The five in-span hinges in the superstructure have a seat width of 0.81 m or 0.91 m. The hinge support of the girders is provided by elastomeric bearing pads. A shear key exists to prevent relative tangential displacement at the hinges. Additionally, new cable restrainers were employed to prevent excessive relative radial displacement leading to unseating.

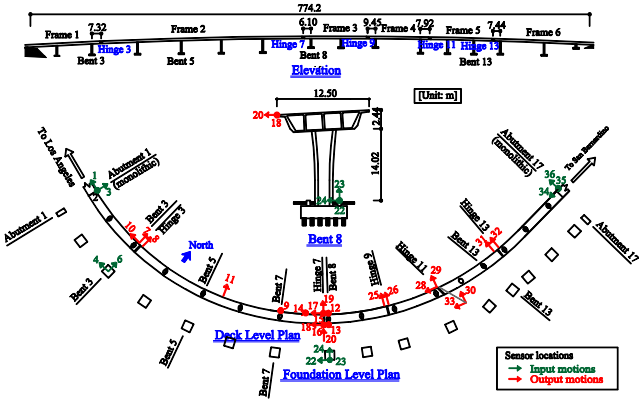

Figure 1: Plan, elevation, and sensor location of the Northwest Connector.

The numerical model of the Northwest Connector is created using OpenSees (McKenna et al. 2010). Since it is expected that the deck would remain elastic during earthquakes, the superstructure is modeled as a spine with elastic beam-column elements. To represent the diaphragms and in-span hinges and to capture the torsion of the box girder due to the bridge curvature, the transverse beam elements are modeled using elastic beam-column elements (rigid and massless). The translational mass is lumped at the nodes of the longitudinal superstructure elements. The torsional mass of inertia about the bridge alignment axis is included to reflect the effect of twisting. An in-span hinge model is developed by combining individual component response models. The effect of pounding is modeled using a nonlinear compression element with the gap model proposed by Muthukumar and DesRoches (2006). The cable restrainer is modeled using a

bilinear tension-only element with an initial slack. Additionally, the nonlinear response of elastomeric bearings is simulated using an elastic-perfectly plastic model based on the shear modulus, height, area, coefficient of friction of the pads, and normal force on the bearing. Columns are modeled using displacement-based beam-column elements along with rigid links at the superstructure-column and footing-column connections. The pile foundations are modeled using lumped springs reflecting the geometry and pile group effect. Moreover, lumped translational springs are used to describe the nonlinear actions of the abutments in the radial and tangential directions.

Comparison between sensor data recorded during the 1992 Landers earthquake (Haddadi et al. 2008) and simulation results is performed to investigate the accuracy of the nonlinear numerical model for the subject complex bridge along with the impact of multi-support motions. Moreover, five percent Rayleigh damping is employed in the simulation. First, uniform excitation analysis is performed for model validation. The ground accelerations at the base of Bent 8 are selected as input motions and are imposed to all of the bases.

A comparison of the recorded and simulated displacement time histories from uniform and multi-support excitation analyses for two sensors is shown in Figure 2: Sensor 7 at Hinge 3 and Sensor 30 at Hinge 11. It is observed that the numerical bridge model using multi-support motions appropriately captures all the responses with regard to amplitude, frequency, and phase compared to the uniform excitation case. The observed results emphasize the importance of multi-support excitation analysis for evaluating the seismic performance of long multi-frame bridges.

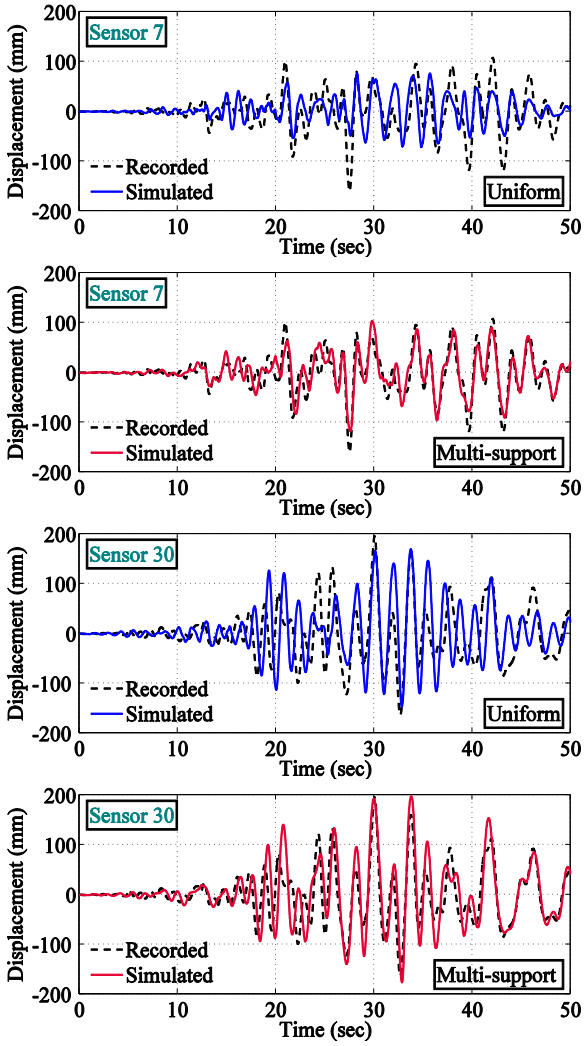

Figure 2: Comparison of recorded and simulated displacement time histories of the bridge.

3. GROUND MOTION SIMULATION

This study follows the approach proposed by Vanmarcke et al. (1993) to simulate different unknown support motions through conditional simulation and a known ground motion at a bridge support. The detailed description of this approach can be found in the reference. This section explains key characteristics of the conditional simulation method used in this study. To simulate non-stationary motions (more realistic ground motions) in which both the frequency content and amplitude evolve with time, the known acceleration time history was divided into m segments with different spectral densities, each of which is considered stationary. The range of each segmented motion is determined based on the amplitude, frequency, and envelope of vibrations. Each power spectral density function (PSD) is estimated in the consecutive time windows using the Burg method (Bos *et al* 2002). This approach fits an

autoregressive model to the signal by minimizing forward and backward prediction errors in the least-squares sense. Each PSD is used to simulate the corresponding stationary segment of the motion, and a non-stationary time history is achieved by piecing the simulated stationary segments together via the linear interpolation algorithm developed by Vanmarcke *et al.* (1993).

Another critical feature is to define the correlation model between known and unknown ground motions. This study adopts the empirical correlation model, $\rho(\omega,r)$, suggested by Loh and Yeh (1988):

$$\rho(\omega, r) = \exp\left[-\frac{\omega r}{2\pi v_s \xi}\right] \quad (1)$$

where v_s is the average shear wave velocity in the soil medium (m/sec) and ξ is a distance scale parameter. While Eq. (1) expresses a simple prediction model, Vanmarcke et al. (1993) stated that the model is consistent with the characteristics of empirical correlation functions obtained from dense accelerograph array data.

To use OpenSees, simulated acceleration time histories are converted into the associated displacement time histories. For this purpose, this study uses the method proposed by Liao and Zerva (2006).

4. SEISMIC FRAGILITY ASSESSMENT

Derivation of system fragility curves

Following the approach developed by Nielson and DesRoches (2007), component fragility curves are estimated by convolving probabilistic seismic demand models (PSDMs) and capacity-based limit state models (*C*). PSDMs are linear regression models in the log-transformed space for seismic demand (*D*)-IM pairs for each component. The fragility function for each component can be expressed as:

$$P_{f,componet} = P[D \geq C \mid IM] = \Phi\left[\frac{\ln(S_D / S_C)}{\sqrt{\beta_{D|IM}^2 + \beta_C^2}}\right] \quad (2)$$

where S_D and S_C are the median value of the seismic demand and structural capacity, respectively, $\beta_{D|IM}$ is the dispersion of the demand conditioned on the IM, and β_C is the dispersion of the capacity. Finally, $\Phi[\bullet]$ is the cumulative normal distribution function.

The bridge system fragility is generated by using a joint probabilistic seismic demand model (JPSDM). This approach implies that there is some level of correlation between individual component demands for a given earthquake, and thus the system demand becomes simply the joint demand on the individual components. The JPSDM is developed in the logarithmic space by employing the transformed marginal distribution of individual components and developing the covariance matrix through the evaluation of the correlation coefficients between the transformed demands. Using the limit state models and the JPSDM, the probability of the system failure is computed across various ranges of the IM using Monte Carlo simulation. In the simulation, the realizations of the demand and capacity are compared to calculate the probabilities of exceeding the limit states of individual components. Ultimately, the results of the integration are in the form of the median and dispersion characterizing the bridge system fragility through a regression analysis:

$$P_{f,system} = P[LS \mid IM] = \Phi\left[\frac{\ln(IM) - \ln(\lambda_i)}{\zeta_i}\right] \quad (3)$$

where λ_i and ζ_i are the median value and dispersion, respectively, of the *i*th limit state.

The derivation of bridge fragility curves includes generation of *N* statistical bridge samples, selection of a suite of *N* ground motions, simulation of *n* support motions for each known motion, generation of PSDMs through the results of NTHAs, definition of limit state models, and derivation of component and system fragility curves.

4.1. Uncertainties in bridge models

Uncertainties in modeling parameters that can affect the component and/or system capacity are

considered in this study. Table 1 presents the probability distributions for each of the above parameters, which are determined based on previous studies (Nielson and DesRoches 2007, Ramanathan 2012). Using the uncertainty in the modeling parameters, statistically significant yet nominally identical bridge models are generated by sampling across the range of these parameters using the Latin hypercube sampling technique.

Table 1: Probability distributions for bridge models.

Random variables	*Units*	*Probability distribution**
Concrete compressive strength	*MPa*	*N(μ = 34.5, COV = 12.5%)*
Rebar yield strength	*MPa*	*LN(μ = 455, COV = 8%)*
Steel jacket yield strength	*MPa*	*N(μ = 276, COV = 10%)*
Shear modulus of bearing	*GPa*	*U (0.55, 1.86)*
Coefficient of friction of bearing	–	*LN(μ = 1.0, COV = 10%)*
Damping ratio	–	*N(μ = 0.045, COV = 27%)*

* N = normal distribution, LN = lognormal distribution, and U = uniform distribution. μ and COV are the mean value and coefficient of variation, respectively, of a random variable.

4.2. Suite of spatially correlated ground motions

Suite of known ground motions

This study chooses the suite of ground motions used in Jeon et al. (2014). This suite consists of 80 ground motions extracted from the PEER Strong Motion Database by Medina and Krawinkler (2003) along with 20 ground motions pertinent to Los Angeles selected from the SAC project database. The 80 PEER ground motions have an even selection of recorded time histories from four bins that include combinations of low and high magnitudes as well as large and small epicentral distances. The 20 SAC ground motions have 10 pairs with 2% and 10% probability of exceedance in 50 years. This suite serves as the known ground motions at a reference source for the generation of spatially varying ground motions at the multiple supports. The reference point is selected as the base of Bent 8, because it is located at the bridge center.

Spatially variable ground motions

Following the procedure proposed by Vanmarcke et al. (1993) that is described in Section 3, unknown ground motions at the location of bridge bents were stochastically generated by conditioning them on the prescribed motions. For the simulation of ground motions, the correlation model in Eq. (1) is first defined. Variables in this correlation model are the target distance (r), distance scale parameter (ξ), and average shear wave velocity (v_s) in the soil medium. This study adopts a distance scale parameter (ξ) of 5. Additionally, the downhole tests at the bridge site conducted by Jackura et al. (1991) provide an estimate of 480 m/sec for the v_s for alluvial sands. Due to insufficient information for each support, this study assumes that the soil profile at the location of the bridge is uniform with a v_s of 480 m/sec. To identify the influence of v_s on simulated motions as well as structural responses, this study also considers four additional soil conditions with v_s values defined in ASCE 7-10 (2010): a v_s of 1150 m/sec for hard rock sites, a v_s of 360 m/sec for dense soil sites, a v_s of 180 m/sec for soft soil sites, and a v_s of 100 m/sec for very loose soft soil. In other words, the degree of correlation is controlled by v_s with the fixed value of ξ. In summary, to identify the effect of v_s values on the response quantities obtained from NTHAs, this study uses r at all supports, a ξ of 5, and five different values of v_s to simulate 16 unknown support motions for each earthquake scenario in the suite of ground motions.

4.3. Demand and capacity models

4.3.1. Engineering demand parameters

To reflect the vulnerability of multiple components, the component responses (the so-called engineering demand parameters (EDPs)) are monitored in analyses. The EDPs are peak column drift (θ_c in %), peak superstructure (opening) deformation (δ_s in mm), and peak bearing shear strain (γ_b in %) as well as peak passive, active, and transverse abutment deformations (δ_p, δ_a, and δ_t in mm). This study

selects the peak response of components of the same type in each sub-frame and in-span hinge location as the EDP value to reduce the post-processing effort and to ensure higher accuracy in the estimation of the probability of failure.

4.3.2. Intensity measure accounting for spatial variation of ground motions

To characterize the correlation model for PGAs, 100 samples of conditional simulations of ground motions for 17 locations in the bridge are generated for a range of v_s. From these results, the correlation matrix ρ_{PGA} of PGAs is derived. It is important to note that each PGA is the geometric mean of two horizontal components. Using the nonlinear least-squares approach, the following exponential decay model is found to provide a reasonable estimate of the spatial correlation of PGAs:

$$\rho_{PGA}(r) = \exp\left[-5.769\times10^{-5}\left(\frac{r}{2\pi v_s \xi}\right)^{0.331}\right] \quad (4)$$

Assuming that IMs for ground motions of various locations are identically distributed and statistically correlated and that they follow a multivariate normal distribution, only a mean, a standard deviation, and a correlation matrix are required to represent the probabilistic model of these random variables. It is assumed that the mean of the PGA of a set of spatially correlated ground motions (μ_{PGA}) could be represented by the PGA of the known ground motion. To determine the standard deviation of the PGAs, the coefficient of variation of PGAs is calculated for 100 sets of 17 ground motions that are conditionally simulated at various locations of the bridge for each v_s. Implementing the nonlinear least-squares approach, the following model is found to appropriately estimate the mean coefficient of variation:

$$\eta_{PGA} = \exp\left(-5.475\times10^{-4} v_s - 2.163\right) \quad (5)$$

Using two sets of relationships for odd- and even-order moments proposed by Bar and Dittrich (1971), the expected value of the products of PGAs at 17 supports can be expressed as:

$$\left(E\left[PGA_1 PGA_2 \cdots PGA_{2n-1}\right]\right)^{\frac{1}{2n-1}} = \left[\sum_{k=1}^{n}\binom{2n-1}{2k-1}\frac{(2n-2k)!}{(n-k)!2^{n-k}}\left(\mu_{PGA}\right)^{2n-1}\left(\eta_{PGA}\right)^{2(n-k)}\right]^{\frac{1}{2n-1}}, \quad (6)$$
$$n = 1,2,3,\cdots,17$$

4.3.3. Limit state models

For the selected EDPs, limit state models also follow a two-parameter lognormal distribution (median and dispersion), as summarized in Table 2. This study uses component limit state models proposed by prior studies: columns, superstructures, and bearings by Jeon et al. (2014) and other components by Ramanathan (2012).

5. SYSTEM FRAGILITY CURVES

As alluded in Section 4.1, bridge system fragility curves are developed using Monte Carlo simulation, one of widely used methods, where realizations of the demand and capacity (limit states) are compared to compute the probabilities of exceeding individual limit states. The lognormal parameters defining the system fragility curves are then estimated based on the

Table 2: Limit state models.

EDPs		*Slight*		*Moderate*		*Extensive*		*Complete*	
		S_C	β_C	S_C	β_C	S_C	β_C	S_C	β_C
Column drift, θ_c (%)		*1.41*	*0.22*	*2.75*	*0.24*	*3.90*	*0.22*	*5.00*	*0.18*
Superstructure deformation δ_s (mm)	*Hinges 3 and 7*	–	–	–	–	*762*	*0.47*	*864*	*0.47*
	Hinges 9 and 11	–	–	–	–	*508*	*0.47*	*762*	*0.47*
	Hinge 13	–	–	–	–	*559*	*0.47*	*762*	*0.47*
Bearing shear strain, γ_b (%)		*100*	*0.35*	*150*	*0.35*	*200*	*0.35*	*350*	*0.35*
Abutment deformation (mm)	*Passive, δ_p*	*76.2*	*0.35*	*254.0*	*0.35*	–	–	–	–
	Active, δ_a	*38.1*	*0.35*	*101.6*	*0.35*	–	–	–	–
	Transverse, δ_t	*25.4*	*0.35*	*101.6*	*0.35*	–	–	–	–

concept of parameter estimation using lognormal probability plotting technique (cumulative density functions). Figure 3 shows the system fragility curves for the bridge using multi-support motions with different v_s. A very minor difference due to the variety of v_s is seen in the curves at the slight limit state, as depicted in Figure 3(a). The system fragility curves for the cases of v_s greater than or equal to 360 m/sec are very similar for all the limit states. However, for the cases of v_s being less than or equal to 180 m/sec, significant differences are observed in the curves at the extensive and complete limit states (see Figure 3(b)). The largest difference is observed between a v_s of 360 m/sec and 180 m/sec which can be recognized as the boundary of dense and soft soils. To further quantify the effect of v_s on the system fragility curves, the median values and dispersions are compared. As mentioned before, the difference between the median values for all the cases of v_s is negligible (within 3% difference in the median value when compared to the case of a v_s of 1150 m/sec) except for the moderate damage state in the case of a v_s of 100 m/sec (about 8% difference). For the extensive and complete damage state, the median values of system fragilities for the cases of a v_s of 360m/sec decrease by at most 6% when compared to the case of a v_s of 1150 m/sec. On the other hand, the medians for the cases of v_s less than or equal to 180 m/sec decrease considerably: a 12~16% reduction in the median value for a v_s of 180 m/sec and a 18~23% reduction in the median value for a v_s of 100 m/sec. Moreover, the system fragility curves using multi-support motions simulated at softer soil sites have a lower value of the dispersion than those at more dense soil sites. In summary, multi-support motions with lower v_s produces more severe damage to the components and system of the bridge when compared to the case of motions with higher v_s. Additionally, spatially correlated ground motions simulated under softer soil conditions ($v_s \leq 180$ m/sec) generally produces higher seismic demands and probabilities of reaching a certain limit state than those at harder soil sites due to smaller spatial correlations and, therefore, larger variations in ground motions at various supports.

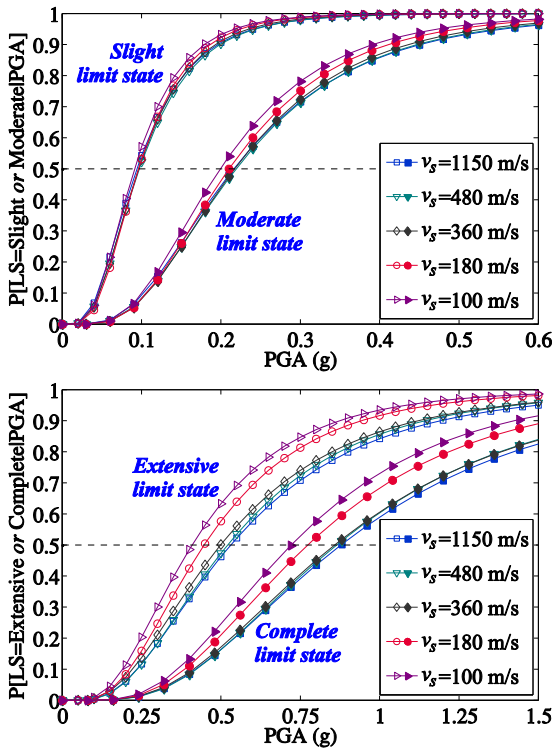

Figure 3: System fragility curves for five shear wave velocities.

6. CONCLUSIONS

This study explored the seismic vulnerability of a long, multi-frame concrete bridge subjected to multi-support ground motions. To accomplish this goal, a numerical bridge model which captures the nonlinear behavior of components is built using OpenSees. The bridge was struck by the 1992 Landers earthquake. To conduct a fragility assessment of the bridge, uncertainty models accounting for different material and structural properties are created. An existing suite of ground motions is employed as a set of known motions to simulate acceleration time histories at multi-supports through a conditional stochastic random process. In this study, the geometric mean of PGAs as an important seismic IM for long multi-frame bridges is proposed to account for the spatial variation of ground motions. The PSDMs for components can be

obtained using the seismic demands monitored in NTHAs and the proposed IM. Finally, system fragility curves are developed using the demand and limit state models and Monte Carlo simulation.

The impact of soil shear wave velocity in a correlation model that characterizes the spatial variation of ground motions on fragility curves is investigated using the results obtained from multiple sets of NTHAs. Looking at the impact on the system fragility, it is observed that the median PGA (system-level) is reduced by approximately 14% for the complete damage state as the shear wave velocity decreases from 1150 m/sec to 180 m/sec. For lower damage states, the impact of spatial variation of ground motions on failure probabilities is less significant. In conclusion, the observed results demonstrated the importance of the proper consideration of the spatial variation of ground motions for large geographically distributed structures such as long multi-frame bridges, particularly at soft soil sites.

7. REFERENCES

ASCE/SEI 7-10 (2010). "Minimum design loads for buildings and other structures (ASCE7-10)." American Society of Civil Engineers, Reston, VA.

Bar, W., and Dittrich, F. (1971). "Useful formula for moment computation of normal random variables with nonzero means." *IEEE Transactions on Automatic Control*, 16(3), 263–265.

Bos, R., de Waele, S., and Broersen, P.M.T. (2002). "Autoregressive spectral estimation by application of the Burg algorithm to irregularly sampled data." *IEEE Transactions on Instrumentation and Measurement*, 51(6), 1289–1294.

Haddadi, H., Shakal, A., Stephens, C., Savage, W., Huang, M., Leith, W., Parrish, J., and Borcherdt, R. (2008). "Center for Engineering Strong-Motion Data (CESMD)." *14th World Conference on Earthquake Engineering*, Beijing, China.

Jackura, K.A., Beddard, D.L., Abghari, A., and Ehsan, J. (1991). "Study of liquefaction potential at the I-10/I-215 interchange in San Bernardino County." California Department of Transportation, Report No. 08-Sbd-10 PM 24.19 & 24.30; E.A. 08-349304, CA.

Jeon, J.-S., Shafieezadeh, A., and DesRoches, R. (2014). "Component fragility assessment of a long, curved multi-frame bridge: Uniform excitation versus spatially correlated ground motions." *Journal of Earthquake Engineering*, in review.

Liao, S., and Zerva, A. (2006). "Physically compliant, conditionally simulated spatially variable seismic ground motions for performance-based design." *Earthquake Engineering and Structural Dynamics*, 35(7), 891–919.

Loh, C.H., and Yeh, Y.T. (1988). "Spatial variation and stochastic modeling of seismic differential ground movement." *Earthquake Engineering and Structural Dynamics*, 16(4), 583–596.

McKenna, F., Scott, M.H., and Fenves, G.L. (2010). "Nonlinear finite-element analysis software architecture using object composition." *Journal of Computing in Civil Engineering*, 24(1), 95–107.

Medina, R.A., and Krawinkler, H. (2003). "Seismic demands for nondeteriorating frame structures and their dependence on ground motions." The John A. Blume Earthquake Engineering Center, Report No. 144, Stanford University, CA.

Muthukumar, S., and DesRoches, R. (2006). "A Hertz contact model with non-linear damping for pounding simulation." *Earthquake Engineering and Structural Dynamics*, 35(7), 811–828.

Nielson, B.G., and DesRoches, R. (2007). "Seismic fragility methodology for highway bridges using a component level approach." *Earthquake Engineering and Structural Dynamics*, 36(6), 823–839.

Ramanathan, K.N. (2012). "Next generation seismic fragility curves for California bridges incorporating the evolution in seismic design philosophy." Georgia Institute of Technology, Atlanta, GA.

Vanmarcke, E.H., Heredia-Zavoni, E., and Fenton, G. (1993). "Conditional simulation of spatially correlated earthquake ground motion." *Journal of Engineering Mechanics*, 119(11), 2333–2352.